09

Generation of unipolar femtosecond pulses of tailored waveform in a layer of atomic hydrogen

© A.V. Pakhomov[1], N.N. Rosanov[1,2], M.V. Arkhipov[1], R.M. Arkhipov[1,2]

[1] St. Petersburg State University,
198504 St. Petersburg, Russia
[2] Ioffe Institute,
194021 St. Petersburg, Russia

e-mail: antpakhom@gmail.com, nnrosanov@mail.ru, mikhail.v.arkhipov@gmail.com, arkhipovrostislav@gmail.com

Received January 15, 2024
Revised January 15, 2024
Accepted January 29, 2024

The possibility to control the temporal electric field profile of unipolar pulses in a multi-level resonant medium is shown when excited by a series of subcycle pulses. The atomic hydrogen was considered as the medium, keeping 5 lowest energy levels in its energy-level structure. Upon the excitation of an optically thick layer of atomic hydrogen by two subcycle attosecond pulses, localized pulses of varying profile were obtained in the layer emission. In particular, unipolar pulses of tailored waveshape and of several femtoseconds in duration, such as rectangular-shaped or triangular-shaped ones, were obtained for certain types of the spatial dependence of the medium density along the layer.

Keywords: few-cycle pulses, electric pulse area, unipolar pulses, light-matter interaction.

DOI: 10.61011/EOS.2024.02.58447.19-24

Introduction

Generation of femtosecond and attosecond impulses, as well as their interaction with various substances is a rapidly developed area of research in the current physics, which attracts more and more attention [1–9]. Such maximally short impulses make it possible to observe the progress of superfast processes up to the intraatomic time scale, including dynamics of individual electrons in atoms, and also allow for relying on the possibility to manage such processes [9–11]. Therefore, the interest in finding new methods to generate and manage the maximally short impulses (primarily in the optical and higher frequency ranges) is quite evident.

The most attractive here is the generation of impulses with the duration of shorter than one cycle of optical oscillations, namely, half-cycle ones. Such impulses contain a single half-wave of electric field, i.e. have a property of unipolarity, that is, the electric field intensity will not change its sign for the entire duration of such impulse. For stricter definition of the unipolar half-cycle impulses it is apparently convenient to introduce such a value as the electric impulse area, which is set with the following expression [12]:

$$\bar{S}_E(\bar{r}) = \int_{-\infty}^{+\infty} \bar{E}(\bar{r}, t')dt', \qquad (1)$$

i.e. it represents a time inteGRal from the electric field strength with infinite integration limits. The electric impulse area (1) has a remarkable conservation property in the unidirectional geometry [12], and also fully determines the impact of maximally short impulses at the quantum systems [13–16].

Recently the methods to produce unipolar subcycle impulses of femtosecond and sub-femtosecond durations are being actively developed [17–22], see also reviews [23,24]. At the same time, the challenge to control the temporal shape of such unipolar impulses seems to be equally important [25,26]. According to the results of the theoretical research, the impact of the unipolar impulses at the quantum objects depends on the impulse shape [27]. Besides, the control of the unipolar impulse shape is important, for example, for their use in management of the states of certain qubits and implementation of the quantum algorithms [28,29]. However, most papers in this area could only achieve the half-cycle impulses, and the question of their temporal shape management was not considered [13,30].

The paper [31] generated a unipolar terahertz impulse in an experimental manner in the form of a precursor of rectangular shape. The recent paper [32] proposed the method to generate unipolar impulses lasting for several femtoseconds with the various temporal profile in the five-level medium of the sodium atoms. Besides, the specific shape of the generated impulse was set by selection of the spatial profile of resonant atom concentration along the atomic sodium layer thickness. Thus, the power form of the concentration profile produced emission of unipolar subcycle impulses of rectangular and triangular shapes.

In this paper we will demonstrate the generation of unipolar impulses in another resonant medium with a different pattern of energy levels, namely, in atomic hydrogen. We will demonstrate the possibility to generate rectangular and triangular unipolar impulses. Besides, we generated the unipolar impulses of a more complicated shape as well when we set other concentration profiles for the resonant atoms in a gas layer. In particular, we considered the non-power shapes of the concentration profiles, which resulted in the emission of unipolar subcycle impulses with a smoother non-monotonic temporal profile of the electric field intensity. Besides, the general approach is described, which enables generation of the unipolar optical impulses of the arbitrary set shape.

Considered model

We consider an optically thick layer of the medium with thickness of L, so that axis z is presumed to be directed normally towards the axis. The layer thickness is considered to be much thicker than the wavelengths of all resonant transitions in the medium. Besides, we will consider the layer to be infinite in transverse directions and review the normal incidence of the linearly polarized exciting impulses, so that the analysis is reduced to the simplest one-dimensional case.

We will consider the atomic hydrogen as a resonant medium, with the parameters of all energy levels and transitions between them being well-known. For more certainty, we will consider 5 lower energy levels of the atomic hydrogen. More specifically, we took the lower 5 levels of the hydrogen atom with the values of the principal quantum number from 1 to 5, i.e. to simplify the calculations, we neglected all mechanisms for splitting of each level in virtue of their comparative smallness vs. the distances of the levels as such. Note that such approach in the dipole approximation enables the transitions between any pair of levels, since actually the degenerate levels are considered, which include all sublevels with different values of the orbital quantum number.

As shown in papers [33,34], upon excitation of the multi-level resonant medium with a pair of linearly polarized half-cycle impulses:

$$E(t) = E_0 e^{-t^2/\tau^2} + E_0 e^{-(t-\pi/\omega_{12})^2/\tau^2}, \qquad (2)$$

the duration of which is shorter than the period of the principal resonant transition $1 \to 2$, while the delay between them is precisely equal to the half of that period, the induced polarization of the medium will be of the form of a half-wave at the frequency of the transition ω_{12}. Besides, the amplitude of the exciting impulses (2) must be such that the populations of the above energy level remain low compared to the population of the first excited level. This was exactly the case in paper [32] to generate the emitted unipolar impulses of non-trivial shape. Below we will consider this particular case, so that the values the exciting half-cycle impulses parameters (2) were chosen based on the condition of the smallness of residual oscillations of the medium polarization after the second of the impulses (2).

To describe the response of the multi-level resonant medium to the field of the exciting impulses, we will use the standard equations for amplitudes of the bound states, which correspond to the expansion factors of the atom wave function by the internal wave functions of the free atom:

$$\psi(\mathbf{r}, t) = \sum_{n=1}^{5} a_n(t)\psi_n(\mathbf{r})e^{-\frac{iE_n t}{\hbar}}, \qquad (3)$$

where $a_n(t)$ — amplitudes of expansion of the atom wave function by the internal wave functions $\psi_n(\mathbf{r})$, E_n — level energy with number n in the energy spectrum of the atom. Then the time dynamics for the amplitudes of the bound states $a_n(t)$ from the expansion (3) is determined by the following equations, which directly proceed from the temporal Schrödinger equation [35]:

$$\dot{a}_n(t) = \frac{i}{\hbar}\sum_{n=1}^{5} d_{nm}a_m(t)E(t)e^{i\omega_{nm}t},$$

$$\omega_{nm} = \frac{E_n - E_m}{\hbar}, \qquad (4)$$

where the following notations are introduced: ω_{nm} — transition frequencies between levels n and m, accordingly, d_{nm} — dipole moments of the corresponding transitions. The parameter values of the equation system (4) for the atomic hydrogen were taken from the manual [36] and are given in the table below.

The induced polarization is expressed via the amplitude of the bound states (4) as

$$P(z, t) = N(z)\sum_{n=1}^{5} d_{nm}a_n(z, t)a_m^*(z, t) + c.c., \qquad (5)$$

where $N(z)$ — the volume concentration of the resonant atoms. Besides, the space-time dynamics of the electric field in the medium is described by the wave equation

$$\frac{\partial^2 E}{\partial z^2} - \frac{1}{c^2}\frac{\partial^2 E}{dt^2} = \frac{4\pi}{c^2}\frac{\partial^2 P}{dt^2}, \qquad (6)$$

where $E(z, t)$ — intensity of the linearly polarized electric field, $P(z, t)$ — induced polarization of the multi-level resonant medium (5) with the spatial dependence of the volume atom concentration $N(z)$, c — velocity of light in vacuum.

Numerical simulation results

Let us consider the emission of the optically thick layer of atomic hydrogen, the parameters of which are given in the table together with the values of the exciting impulses parameters (2). To calculate the emitted field, the simultaneous numerical solution of the wave equation (6) was

Transition frequencies and effective dipole moments for the first 5 levels of atomic hydrogen, as well as parameters of exciting impulses and the medium layer

Duration of exciting impulses	$\tau = 30\,\text{as}$
Amplitude of exciting impulses	$E_0 = 10^5\,\text{CGS units}$
Maximum value of volume concentration of atoms in the layer	$N_0 = 2.7 \cdot 10^{19}\,\text{cm}^{-3}$
Thickness of the medium layer	$L = 3\,\mu\text{m}$
Transition frequency $1 \to 2$	$\omega_{12} = 1.55 \cdot 10^{16}\,\text{rad/s}$
Dipole transition moment $1 \to 2$	$d_{12} = 3.27\,\text{D}$
Transition frequency $1 \to 3$	$\omega_{13} = 1.84 \cdot 10^{16}\,\text{rad/s}$
Dipole transition moment $1 \to 3$	$d_{13} = 1.31\,\text{D}$
Transition frequency $1 \to 4$	$\omega_{14} = 1.94 \cdot 10^{16}\,\text{rad/s}$
Dipole transition moment $1 \to 4$	$d_{14} = 0.77\,\text{D}$
Transition frequency $1 \to 5$	$\omega_{15} = 1.98 \cdot 10^{16}\,\text{rad/s}$
Dipole transition moment $1 \to 5$	$d_{15} = 0.53\,\text{D}$
Transition frequency $2 \to 3$	$\omega_{23} = 2.87 \cdot 10^{15}\,\text{rad/s}$
Dipole transition moment $2 \to 3$	$d_{23} = 12.63\,\text{D}$
Transition frequency $2 \to 4$	$\omega_{24} = 3.88 \cdot 10^{15}\,\text{rad/s}$
Dipole transition moment $2 \to 4$	$d_{24} = 4.85\,\text{D}$
Transition frequency $2 \to 5$	$\omega_{25} = 4.34 \cdot 10^{15}\,\text{rad/s}$
Dipole transition moment $2 \to 5$	$d_{25} = 2.83\,\text{D}$
Transition frequency $3 \to 4$	$\omega_{34} = 1.01 \cdot 10^{15}\,\text{rad/s}$
Dipole transition moment $3 \to 4$	$d_{34} = 29.33\,\text{D}$
Transition frequency $3 \to 5$	$\omega_{35} = 1.47 \cdot 10^{15}\,\text{rad/s}$
Dipole transition moment $3 \to 5$	$d_{35} = 10.76\,\text{D}$
Transition frequency $4 \to 5$	$\omega_{45} = 4.63 \cdot 10^{14}\,\text{rad/s}$
Dipole transition moment $4 \to 5$	$d_{45} = 29.93\,\text{D}$

implemented by the finite-difference time-domain method (FDTD — finite-difference time-domain), while for the medium response, the equations were solved numerically for the amplitudes of the bound state (4) by Runge–Kutta method of the 4th order. Let us first consider the case of the power function of the atom concentration profile $N(z)$. In particular, we will take the concentration profile of the following piecewise-power form:

$$N(z) = N_0 \frac{3z}{L}, \qquad 0 \le z \le \frac{L}{3},$$

$$N(z) = N_0, \qquad \frac{L}{3} \le z \le \frac{2L}{3},$$

$$N(z) = N_0 \frac{9(L-z)^2}{L^2} \qquad \frac{2L}{3} \le z \le L. \qquad (7)$$

In this case the concentration profile is linear and quadratic at the edges, accordingly, while in the central part the concentration is constant. According to the results of paper [32], at such concentration profile (7) the emitted field must include a pair of unipolar impulses of various polarity, besides, the first of them must have the rectangular shape, and the second one — the triangular one.

The estimated time dependence of the electric field in reflection from the layer is shown in Fig. 1. As can be seen, in the reflection the rectangular and the triangular unipolar impulses of opposite polarity are produced indeed. Besides, the electric area (1) of the entire emitted field turns out to be equal to zero. Both unipolar impulses follow with a time delay, which is determined by the length of the central part of the concentration profile (7) with the constant value. Fast oscillations of the field in the background that are well-visible in Fig. 1, *b*, are due to the contribution of the above energy levels in the considered multi-level medium.

Let us then take the non-power form of the atom concentration profile $N(z)$. Let the concentration profile be of the following form close to the stepped one:

$$N(z) = \frac{N_0}{4}\left(1 + \tanh\left[\frac{z - z_1}{h}\right]\right)\left(1 + \tanh\left[\frac{z_2 - z}{h}\right]\right)$$

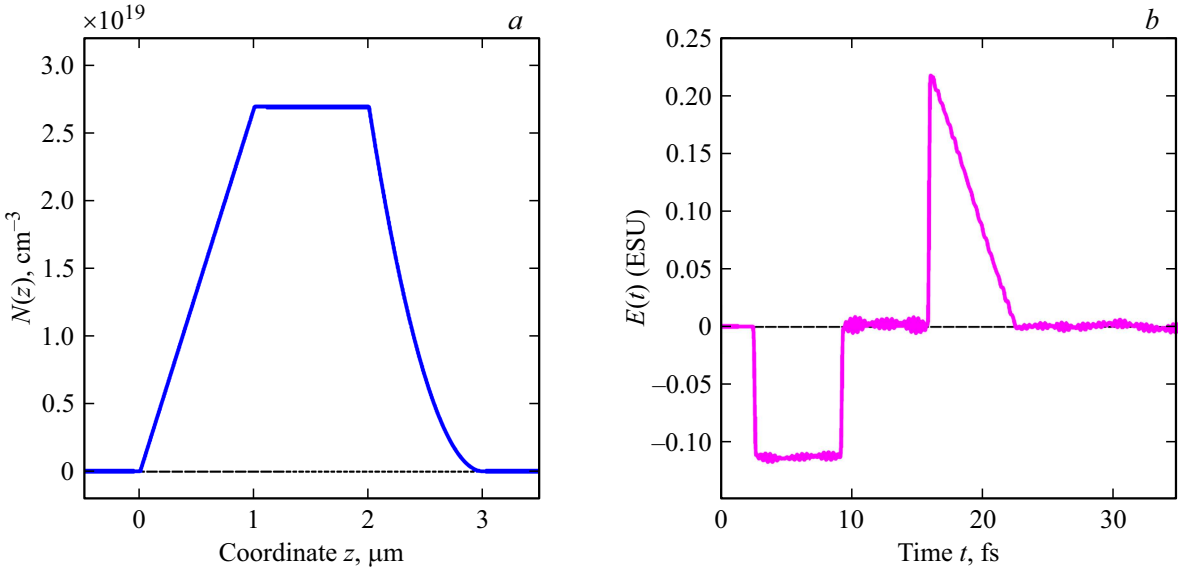

Figure 1. Emission of the atomic hydrogen layer with thickness of $L = 3\,\mu$m at pressure of 1 at and upon excitation with a pair of sub-cycle unipolar impulses (2) with duration $\tau = 30$ as and amplitude $E_0 = 10^5$ units CGS: (a) profile of volume concentration of atoms $N(z)$, set by the expression (7); (b) emitted field in the reflection.

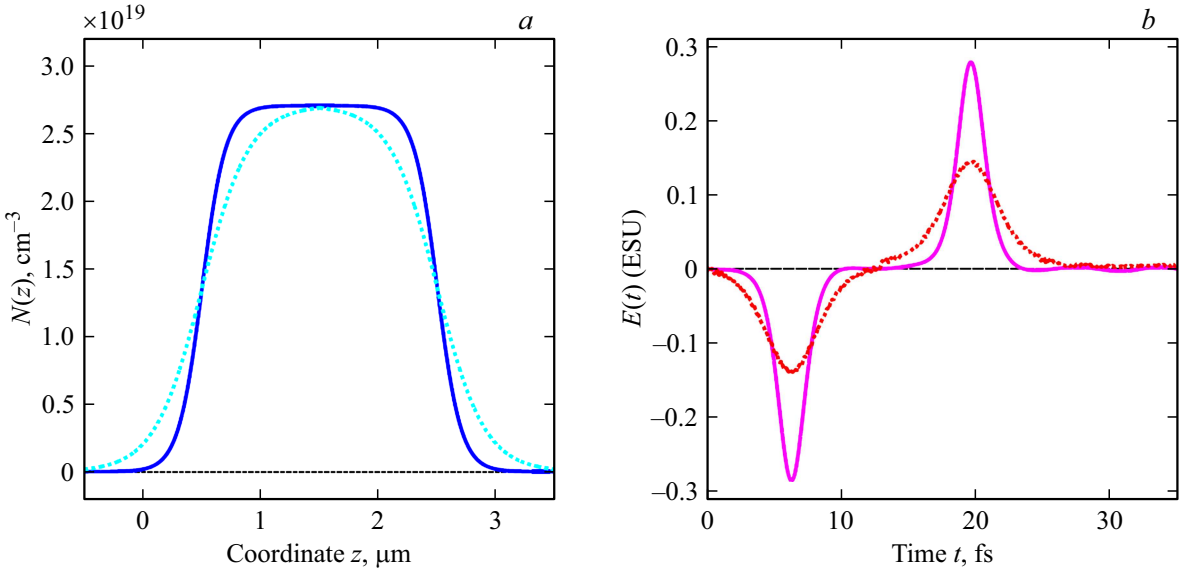

Figure 2. Emission of the atomic hydrogen layer with thickness of $L = 3\,\mu$m at pressure of 1 at and upon excitation with a pair of sub-cycle unipolar impulses (2) with duration $\tau = 30$ as and amplitude $E_0 = 10^5$ CGS units: (a) profile of volume concentration of atoms $N(z)$, set by the expression (8) at $h = 400$ nm (dotted line) and $h = 200$ nm (solid line); (b) emitted field in reflection at $h = 400$ nm (dotted line) and $h = 200$ nm (solid line).

$$z_1 = 0.5\,\mu\text{m}, \qquad z_2 = 2.5\,\mu\text{m}, \tag{8}$$

where parameter h determines the specific thickness of the profile borders. Besides, in the central part the atom concentration is again actually constant and equal to the maximum value N_0. The results of the numerical simulation for the concentration profile of form (8) and for several values of the quantity h are shown in Fig. 2.

As can be seen from Fig. 2, in this case two bell-shaped unipolar impulses are generated. Besides, the more smoothed is the concentration profile (8), the less is the amplitude, and the longer is the duration of the produced unipolar impulses. Let us note that the unipolar impulses generated in this case have the symmetrical shape. This is due to the fact that the shape of the side borders of the concentration profile (8) is symmetrical relative to points z_1 and z_2.

Let us consider for comparison another shape of the concentration profile $N(z)$, which does not have such

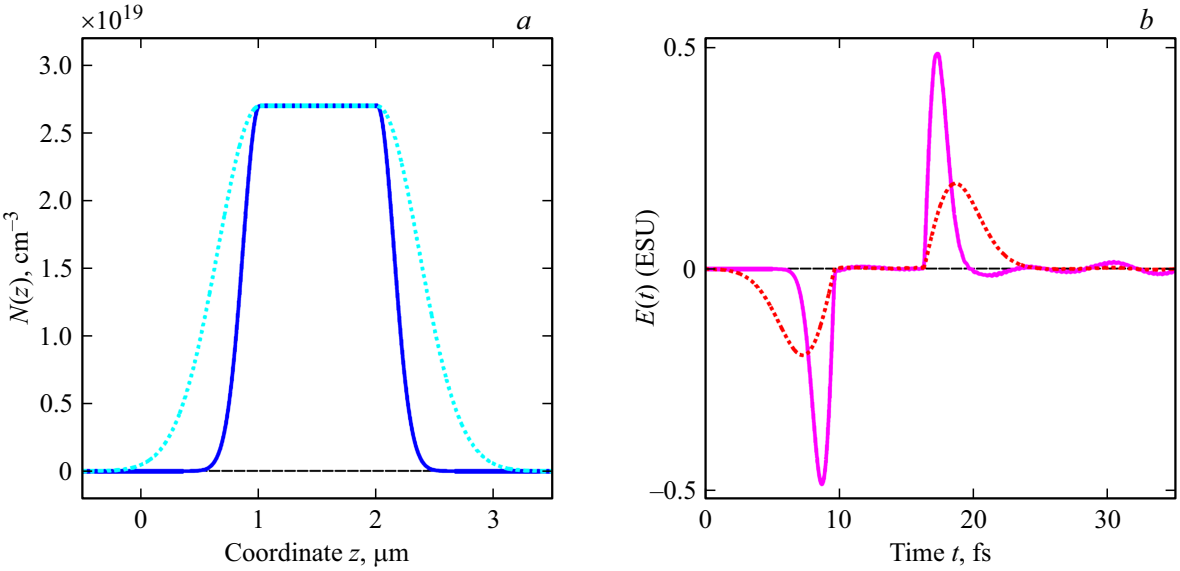

Figure 3. Emission of the atomic hydrogen layer with thickness of $L = 3\,\mu$m at pressure of 1 at and upon excitation with a pair of sub-cycle unipolar impulses (2) with duration $\tau = 30$ as and amplitude $E_0 = 10^5$ CGS units: (*a*) profile of volume concentration of atoms $N(z)$, set by the expression (9) at $w = 200$ nm (solid line) and $w = 500$ nm (dotted line); (*b*) emitted field in reflection at $w = 200$ nm (solid line) and $w = 500$ nm (dotted line).

symmetry. For this purpose we suggest the dependence of the volume concentration on the coordinate of the following type:

$$N(z) = N_0 e^{-\left(z-\frac{L}{3}\right)^2/w^2}, \qquad z \le \frac{L}{3},$$

$$N(z) = N_0, \qquad \frac{L}{3} \le z \le \frac{2L}{3},$$

$$N(z) = N_0 e^{-\left(\frac{2L}{3}-z\right)^2/w^2}, \qquad \frac{2L}{3} \le z, \qquad (9)$$

where value w is the thickness of the concentration profile borders $N(z)$. The unipolar impulses emitted by the gas layer with the concentration profile (9), are built in Fig. 3 for various values of parameter w.

The generated unipolar impulses in Fig. 3 have a pronounced asymmetric shape: with a sharper leading front and a smoother trailing front. Such type of the generated impulses directly follows from the asymmetric nature of the selected concentration profile (9). Note that as in the previous case, when transitioning to the smoother shape of the concentration profile (9) the duration of the generated unipolar impulses increases, while the amplitude accordingly decreases.

Generation of the unipolar impulses of the specified shape

Let us now turn to the issue of how a pair of the unipolar subcycle impulses of a certain preset shape may be generated in the emission from the medium layer. Following the review in paper [32], we will assume that the emitted field from each infinitely thin layer of atoms with thickness of dz represents approximately one period of the sine wave at the frequency of the principal transition ω_{12}. Let us further assume that the field is registered in the reflection with a detector located at the distance of D from the left border of the gas layer. In such case with the concentration profile in the layer $N(z)$ the total emission from the entire layer will represent the imposition of emissions from each part of the layer and will be determined by the following equation [32]:

$$E_{\text{emit}}(-D,t) = \int_0^L N(z) A_0 \sin\omega_{12}\left(t - \frac{2z+D}{c}\right) \times \Theta\left(t - \frac{2z+D}{c}\right)\Theta\left(\frac{2z+d}{c} + T_{12} - t\right) dz, \quad (10)$$

where A_0 — the proportionality coefficient, $T_{12} = 2\pi/\omega_{12}$ — the period of resonant transition at the principal resonant frequency, Θ — the Heaviside step function. In expression (10) it is assumed that the first of the exciting half-cycle impulses (2) enters the medium layer at moment of time $t = 0$. In time interval

$$T_{12} + \frac{D}{c} \le t \le \frac{2L+D}{c},$$

, i.e. when both exciting impulses are inside the medium layer, integral (10) is reduced to the view

$$E_{\text{emin}}(-D,t) = \int_{(ct-cT_{12}-D)/2}^{(ct-D)/2} A_0 N(z) \sin\omega_{12}\left(t - \frac{2z+D}{c}\right) dz. \quad (11)$$

. The produced equation (11) makes it possible to consider the inverse problem, i.e. determine the required form of the volume concentration profile $N(z)$ for generation of a certain subcycle impulse of the set form.

The integral in the right part of expression (11) may be calculated explicitly in case of power function $N(z)$. Thus, as shown in papers [37,38], for the constant concentration $N(z) = \text{const}$ integral (11) is equal to zero, in case of linear dependence $N(z) \sim z$ integral (11) is equal to the constant and does not depend on t, and in case of quadratic dependence $N(z) \sim z^2$ the registered field linearly depends on time, $E_{\text{emit}}(-D, t) \sim t$. It can easily be obtained from expression (11), that in case of random power dependence $N(z) \sim z^n$ for the emitted field $E_{\text{emit}}(-D, t)$ the power dependence on time is also obtained, but with the leading summand $\sim t^{n-1}$.

Let us now consider a more general case of the inverse problem, when the field measured by the detector must have the set form $E_{\text{emit}}(-D, t)$. Let us apply the expansion of this function in the Taylor's series:

$$E_{\text{emit}}(-D, t) = e_0 + e_1 t + e_2 t^2 + e_3 t^3 + \ldots \qquad (12)$$

We will treat the unknown function of the volume concentration $N(z)$ in the same manner:

$$N(z) = n_0 + n_1 z + n_2 z^2 + n_3 z^3 + \ldots \qquad (13)$$

In this case the problem of determining the concentration profile $N(z)$ using the set function $E_{\text{emit}}(-D, t)$ is reduced to finding the expansion factors n_0, n_1, n_2, n_3, ... by the known factors e_0, e_1, e_2, e_3, ...

Let us assume that in the expansion (12) of the set field $E_{\text{emit}}(-D, t)$ the members up to the number K are retained. In this case the solution sought for the concentration profile $N(z)$ must be sought in the form (13), where the summands are retained up to $n_{K+1} z^{K+1}$. Calculating then the integral in the right part of the expression (11) using the expansion (13), we obtain the system of linear algebraic equations to determine the unknowns n_0, n_1, n_2, n_3, ..., n_{K+1}. Using the described general algorithm, we can obtain the necessary solution for $N(z)$ with any specified accuracy, increasing the number of the retained summands in the expansion (12) and thus increasing the precision of approximation.

Conclusion

Therefore, the paper theoretically studied the issue of the multi-level medium layer excitation, namely, of atomic hydrogen, with a pair of maximally short impulses with a time delay between them selected in a certain manner. Besides, the duration of the exciting impulses was assumed to be less than the periods of resonant transitions in the medium, and the volume concentration of atoms varied along the thickness of the medium layer.

The completed analysis demonstrated that in such case the layer of the resonant medium emits a pair of unipolar impulses of various polarity, besides, the form of the temporal profile of such impulses may vary. In case of the symmetrical profile of the volume concentration of atoms, two unipolar impulses of identical shape, but with the different sign of the field are generated. In case of the asymmetric profile of the volume concentration of atoms, two unipolar impulses of different form are generated, but in all cases with the zero value of the total electric area (1) of the entire emitted field.

The simplest power forms of the concentration profiles, as well as some more complicated non-power dependences were studied. As a result, both unipolar sub-cycle impulses of rectangular and triangular temporal profiles and unipolar impulses with different non-trivial temporal profiles of the electric field intensity of both symmetric and pronounced asymmetric form were detected. Moreover, based on the completed calculations, the general algorithm was formulated to find the profile of the volume concentration of resonant atoms, when the unipolar impulses of the specified shape are generated.

The obtained results are of theoretical nature and may be experimentally implemented, for example, when a flat gas jet flows through the nozzle of certain geometry. In such case downstream the nozzle, the necessary heterogeneous distribution of the volume concentration of gas atoms may be generated in the direction orthogonal to the direction of the gas jet flow. Note that attosecond half-cycle impulses (2), which were used in the calculations to excite the resonant medium, may currently be produced by the experimentally different methods [17–22]. The obtained results may therefore promote development of the methods to manage the temporal profile of subcycle impulses with the duration of the femtosecond unit order.

Funding

The work has been funded by a grant of the Russian Science Foundation (RSF) № 21-72-10028.

Conflict of interest

The authors declare that they have no conflict of interest.

References

[1] F. Krausz, M. Ivanov. Rev. Mod. Phys., **81**, 163 (2009).
[2] L. Gallmann, C. Cirelli, U. Keller. Ann. Rev. Phys. Chem., **63**, 447 (2012).
[3] M. Chini, K. Zhao, Z. Chang. Nature Photonics, **8**, 178 (2014).
[4] G. Mourou. Rev. Mod. Phys., **91**, 030501 (2019).
[5] J. Biegert, F. Calegari, N. Dudovich, F. Quere, M. Vrakking. J. Phys. B., **54**, 070201 (2021).
[6] B. Xue, K. Midorikawa, E.J. Takahashi. Optica, **9**, 360 (2022).
[7] K. Midorikawa. Nature Photonics, **16**, 267 (2022).
[8] S.V. Sazonov. Opt. Spectrosc., **130**(12), 1573 (2022).
[9] M.Yu. Ryabikin, M.Yu. Emelin, V.V. Strelkov. Phys. Usp., **66**, 360 (2023).

[10] D. Hui, H. Alqattan, S. Yamada, V. Pervak, K. Yabana, M. Hassan. Nature Photonics, **16**, 33 (2022).
[11] K. Ramasesha, S.R. Leone, D.M. Neumark. Annu. Rev. Phys. Chem., **67**, 41 (2016).
[12] N.N. Rosanov. Opt. Spectrosc., **107**, 721 (2009).
[13] M.T. Hassan, T.T. Luu, A. Moulet, O. Raskazovskaya, P. Zhokhov, M. Garg, N. Karpowicz, A.M. Zheltikov, V. Pervak, F. Krausz, E. Goulielmakis. Nature, **530**, 66 (2016).
[14] R.M. Arkhipov, A.V. Pakhomov, M.V. Arkhipov, I. Babushkin, A. Demircan, U. Morgner, N.N. Rosanov. Opt. Lett., **44**, 1202 (2019).
[15] N. Rosanov, D. Tumakov, M. Arkhipov, R. Arkhipov. Phys. Rev. A, **104**, 063101 (2021).
[16] A. Pakhomov, M. Arkhipov, N. Rosanov, R. Arkhipov. Phys. Rev. A, **105**, 043103 (2022).
[17] H.-C. Wu, J. Meyer-ter Vehn. Nature Photonics, **6**, 304 (2012).
[18] J. Xu, B. Shen, X. Zhang, Yin Shi, L. Ji, L. Zhang, T. Xu, W. Wang, X. Zhao, Zh. Xu. Sci. Rep., **8**, 2669 (2018).
[19] Y. Shou, R. Hu, Z. Gong, J. Yu, J. Chen, G. Mourou, X. Yan, W. Ma. New J. Phys., **23**, 053003 (2021).
[20] R. Pang, Y. Wang, X. Yan, B. Eliasson. Phys. Rev. Appl., **18**, 024024 (2022).
[21] S. Wei, Y. Wang, X. Yan, B. Eliasson. Phys. Rev. E, **106**, 025203 (2022).
[22] Q. Xin, Y. Wang, X. Yan, B. Eliasson. Phys. Rev. E, **107**, 035201 (2023).
[23] R.M. Arkhipov, M.V. Arkhipov, A.V. Pakhomov, P.A. Obraztsov, N.N. Rosanov. JETP Lett., **117**, 8 (2023).
[24] N.N. Rosanov. Phys. Uspekhi, **66**, 1059 (2023).
[25] G. Cirmi, R.E. Mainz, M.A. Silva-Toledo, F. Scheiba, H. Çankaya, M. Kubullek, G.M. Rossi, F.X. Kärtner. Laser & Photonics Rev., **17**(4), 2200588 (2023).
[26] R.E. Mainz, G.M. Rossi, F. Scheiba, M.A. Silva-Toledo, Y. Yang, G. Cirmi, F.X. K?rtner. Optics Express, **31**, 11363−11394 (2023).
[27] R. Arkhipov, A. Pakhomov, M. Arkhipov, A. Demircan, U. Morgner, N. Rosanov, I. Babushkin. Optics Express, **28** (11), 17020 (2022).
[28] M.V. Bastrakova, N.V. Klenov, A.M. Satanin. Phys. Solid State, **61**, 1515 (2019).
[29] M.V. Bastrakova, N.V. Klenov, A.M. Satanin. JETP, **131**, 507 (2020).
[30] H. Alqattan, D. Hui, V. Pervak, M.T. Hassan. APL Photonics, **7**, 041301 (2022).
[31] I.E. Ilyakov, B.V. Shishkin, E.S. Efimenko, S.B. Bodrov, M.I. Bakunov. Optics Express, **30**, 14978 (2022).
[32] A. Pakhomov, N. Rosanov, M. Arkhipov, R. Arkhipov. Opt. Lett., **48**, 6504 (2023).
[33] A. Pakhomov, N. Rosanov, M. Arkhipov, R. Arkhipov. J. Opt. Soc. Am. B, **41**, 46 (2024).
[34] R.M. Arkhipov, A.V. Pakhomov, M.V. Arkhipov, N.N. Rosanov. Opt. Spectrosc., **131**(1), 73 (2023).
[35] A. Yariv. *Quantum electronics* (Wiley, NY., 1989).
[36] S.E. Frish. *Opticheskie spektry atomov* (Gos. izdat. fiz.-mat. lit., M.-L., 1963). (in Russian)
[37] A. Pakhomov, M. Arkhipov, N. Rosanov, R. Arkhipov. Phys. Rev. A, **106**, 053506 (2022).
[38] R.M. Arkhipov, M.V. Arkhipov, A.V. Pakhomov, O.O. Diachkova, N.N. Rosanov. JETP Lett., **117**(8), 574 (2023).

Translated by M.Verenikina